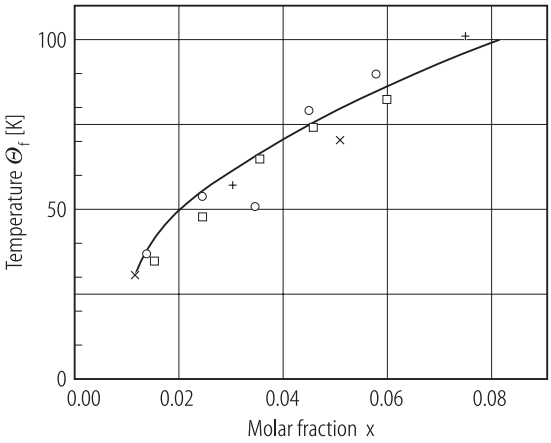

Fig. 1A-5-001. $K_{1-x}Li_xTaO_3$ ($x \leq 0.08$). Θ_f vs. x [92Gli].
x: molar fraction of Li.

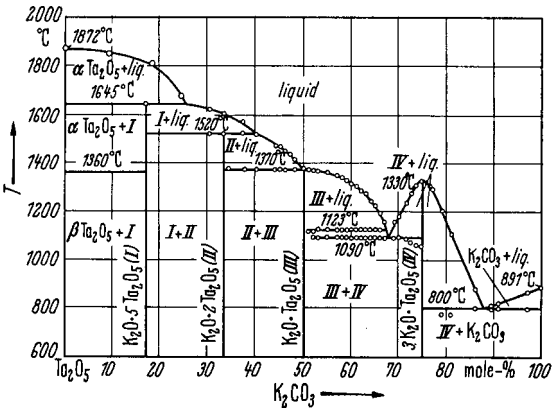

Fig. 1A-5-002. $KTaO_3$. Phase diagram of K_2CO_3–Ta_2O_5 system [56Rei].

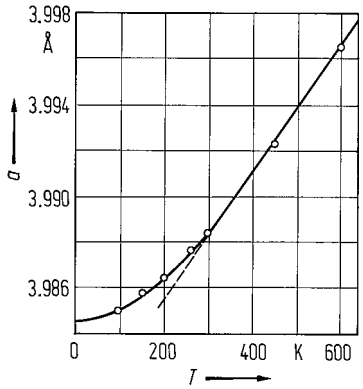

Fig. 1A-5-003. $KTaO_3$. *a* vs. *T* [73Sam]. *a*: unit cell parameter.

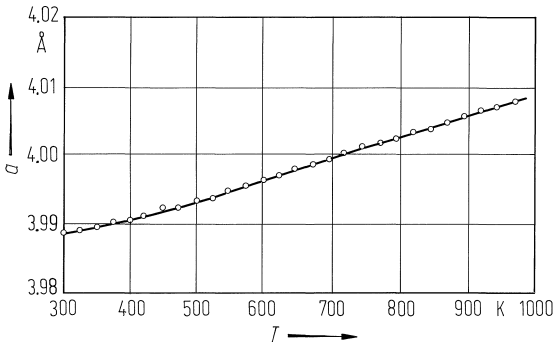

Fig. 1A-5-004. $KTaO_3$. *a* vs. *T* [83Iva]. *a*: unit cell parameter.

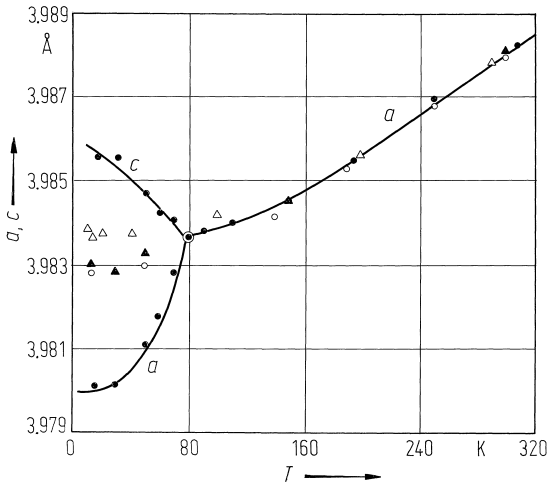

Fig. 1A-5-005. $KTaO_3$, $KTaO_3$:Li, $KTaO_3$:Nb. Unit cell parameters vs. *T* [85And]. Open circles: pure $KTaO_3$, open triangles: 1.7% Nb doped, full triangles: 1.6% Li doped and full circles: 5% Li doped $KTaO_3$ (tetragonal below Θ_t).

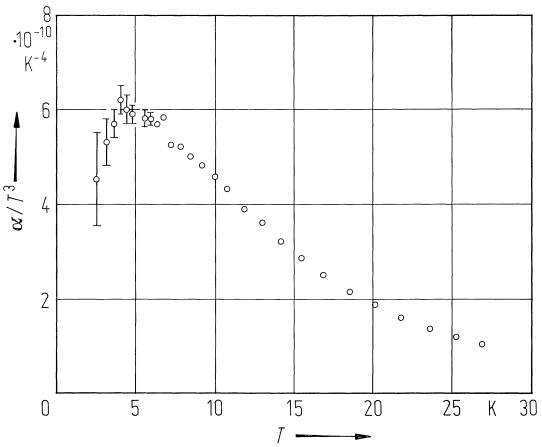

Fig. 1A-5-006. $KTaO_3$. α/T^3 vs. T [81Whi]. α: linear thermal expansion coefficient.

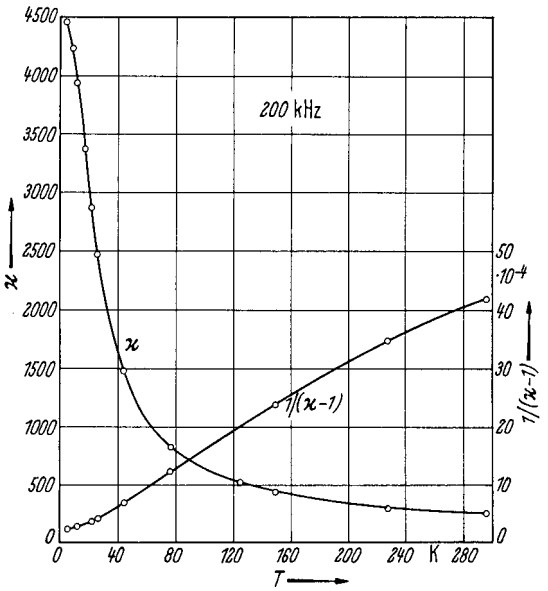

Fig. 1A-5-007. $KTaO_3$. κ, $1/(\kappa - 1)$ vs. T [65Wem].

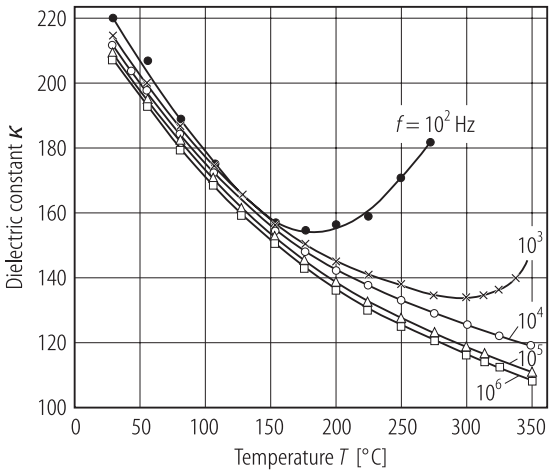

Fig. 1A-5-008. $KTaO_3$. κ vs. T [77Law]. Parameter: f.

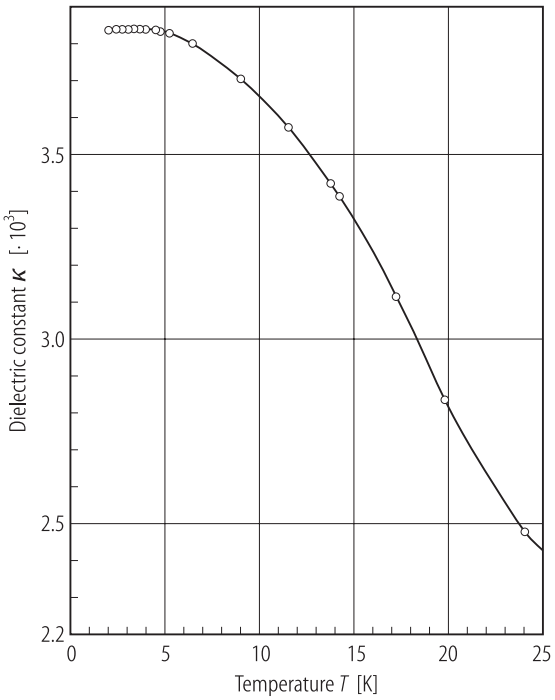

Fig. 1A-5-009. $KTaO_3$. κ vs. T [70Agr]. f = 1 kHz.

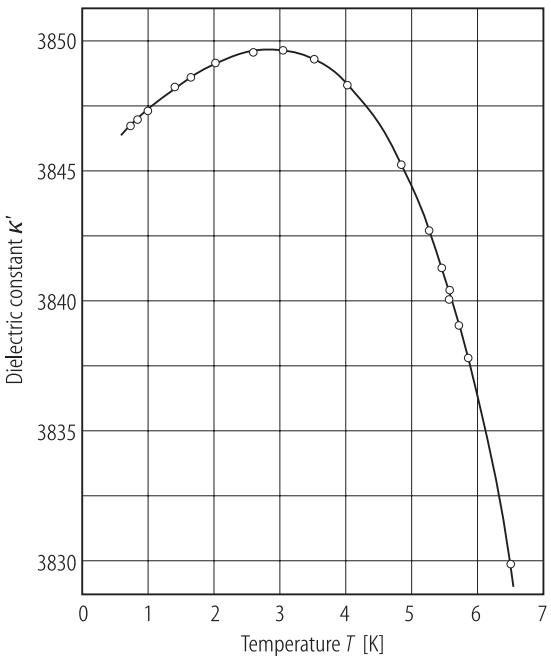

Fig. 1A-5-010. $KTaO_3$. κ' vs. T [76Sie]. f = 1 kHz.

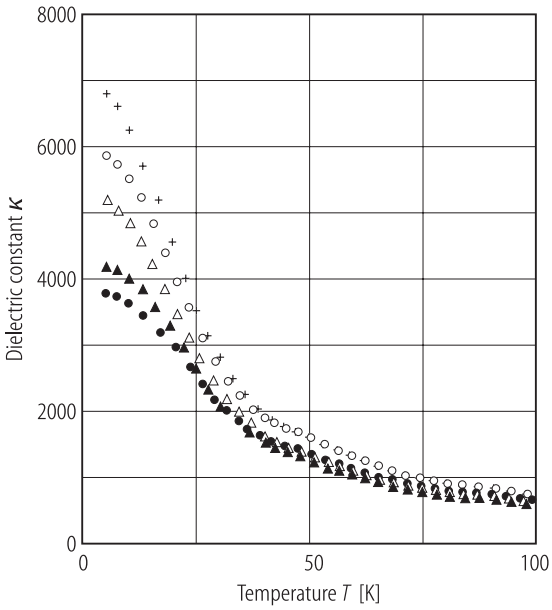

Fig. 1A-5-011. $KTaO_3$, $KTaO_3$:Nb, $KTaO_3$:Na. κ vs. T [94Sal]. f = 1 kHz. Full circles, full triangles: undoped $KTaO_3$; open triangles: 0.15% Nb doped; crosses: > 0.1% Nb doped; open circles: 1% Na doped.

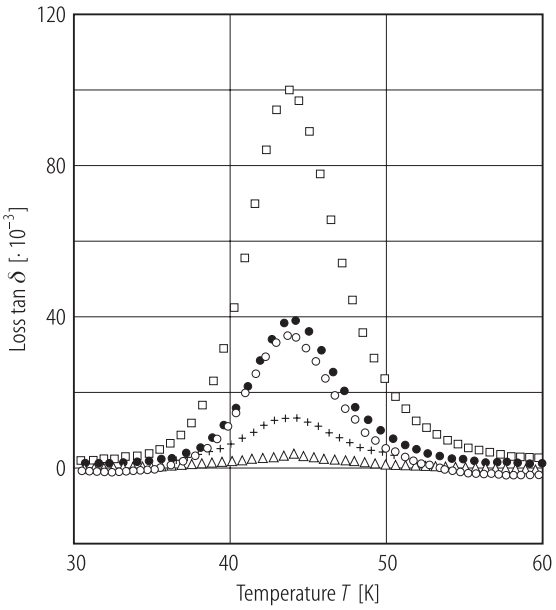

Fig. 1A-5-012. $KTaO_3$, $KTaO_3$:Nb, $KTaO_3$:Na, $KTaO_3$:Fe. tan δ vs. T [94Sal]. δ: dielectric loss angle. f = 1 kHz. Full cicles: undoped $KTaO_3$; open triangles: 0.15% Nb doped; crosses: > 0.1% Nb doped; open circles: 1% Na doped; open spuares: 1% Fe doped.

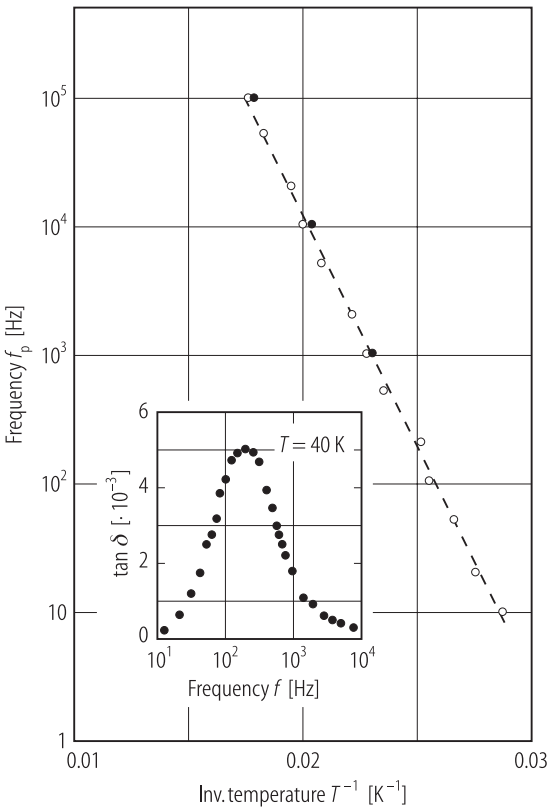

Fig. 1A-5-013. $KTaO_3$. f_p vs. T^{-1} [94Sal]. f_p: frequency at which $\tan\delta$ shows peak. Open circles: undoped $KTaO_3$; full circles: 1% Fe doped. Insert: $\tan\delta$ vs. f for undoped sample at 40 K.

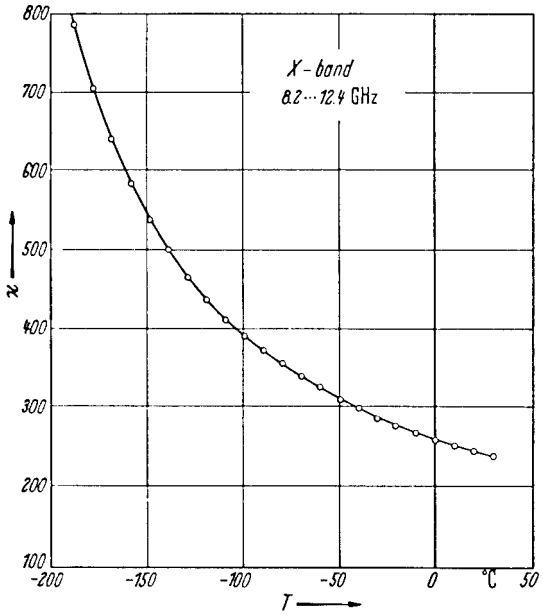

Fig. 1A-5-014. $KTaO_3$. κ vs. T in the range of 8.2...12.4 GHz [64Rup].

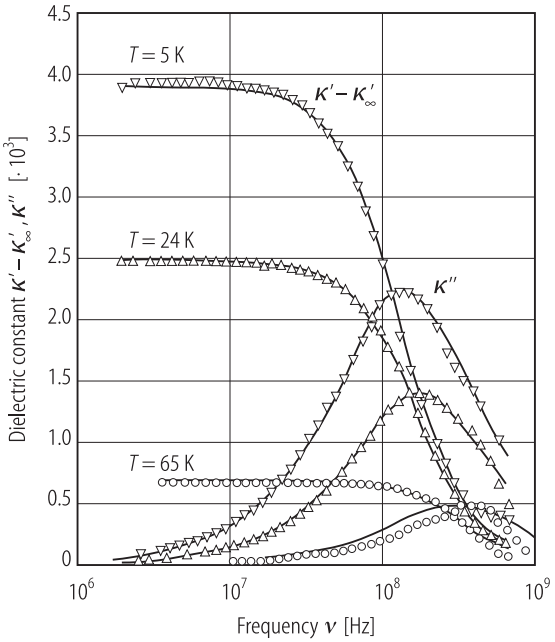

Fig. 1A-5-015. $KTaO_3$. $\kappa' - \kappa'_\infty$, κ'' vs. ν [87Mag]. Parameter: T. $\kappa'_\infty \approx 400$ at $T = 5$ K, dielectric constant in the infrared region.

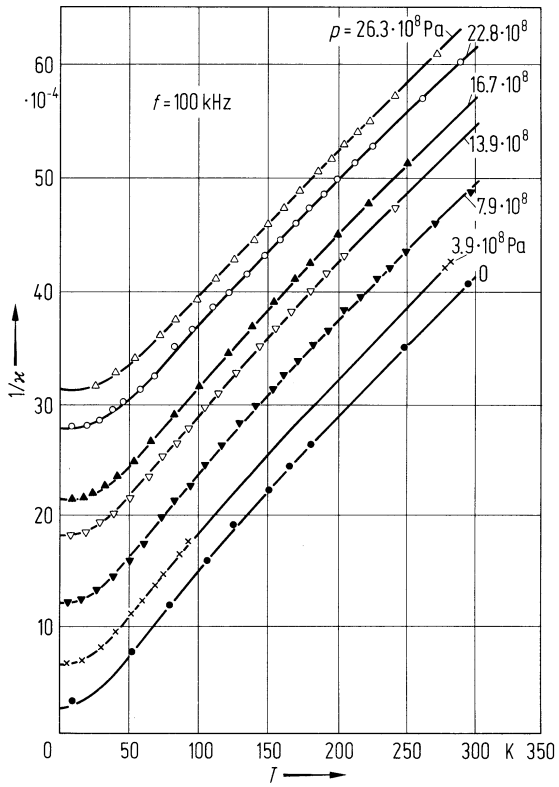

Fig. 1A-5-016. $KTaO_3$. $1/\kappa$ vs. T [71Abe]. Parameter: p.

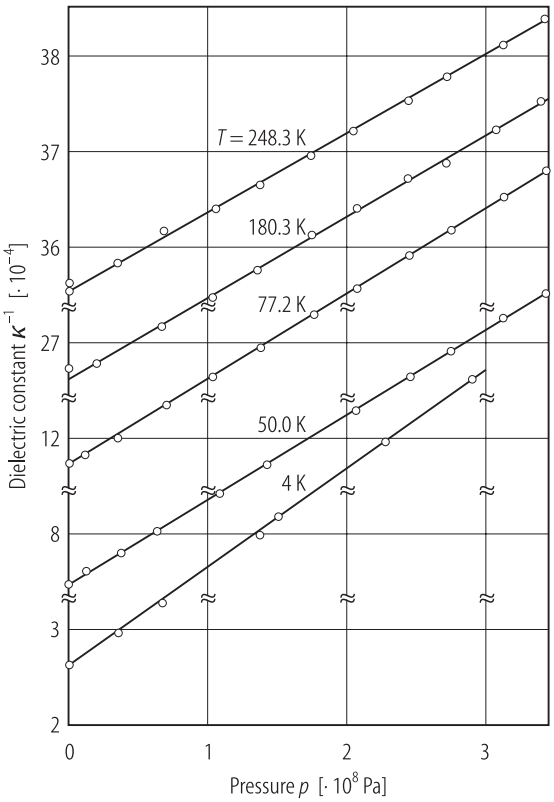

Fig. 1A-5-017. $KTaO_3$. κ^{-1} vs. p [71Abe]. p: hydrostatic pressure. Parameter: T. f = 100 kHz.

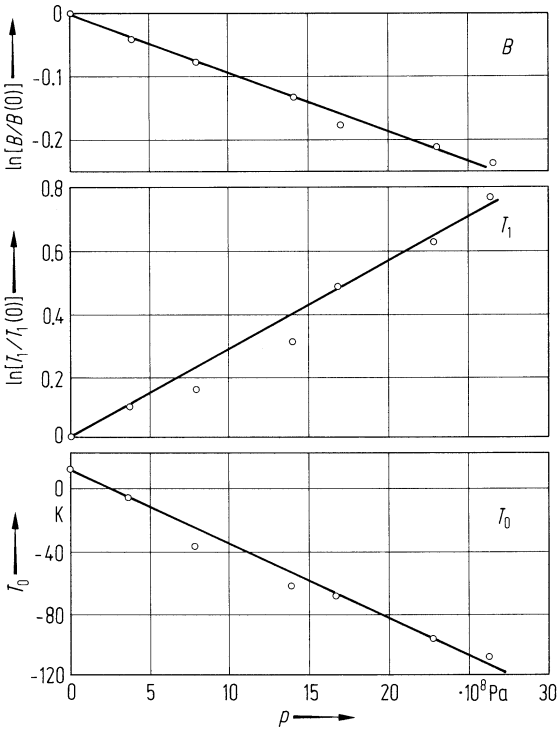

Fig. 1A-5-018. $KTaO_3$. T_0, $\ln[T_1/T_1(0)]$, $\ln[B/B(0)]$ vs. p [71Abe]. Temperature dependence of κ at constant p is represented by $\kappa = B/[(1/2)T_1\coth(T_1/2T) - T_0]$. B, T_1, T_0: emperically determined constants.

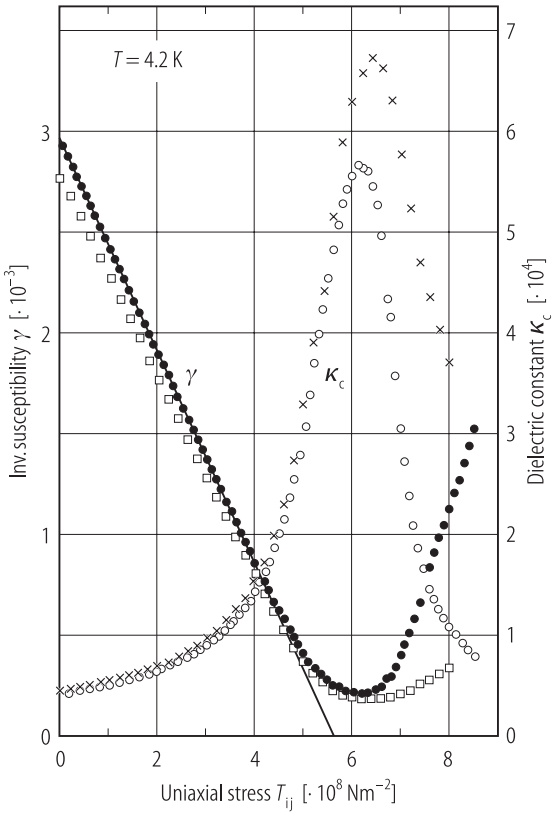

Fig. 1A-5-019. $KTaO_3$. γ, κ_c vs. T_{ij} [75Uwe]. $\gamma = 4\pi / (\kappa_c - 1)$; inverse susceptibility in cgs units. T_{ij}: uniaxial stress. T = 4.2 K. (Open squares, crosses): stress normal to (010) face, (full and open circles): stress normal to (110) face. f = 1...100 kHz.

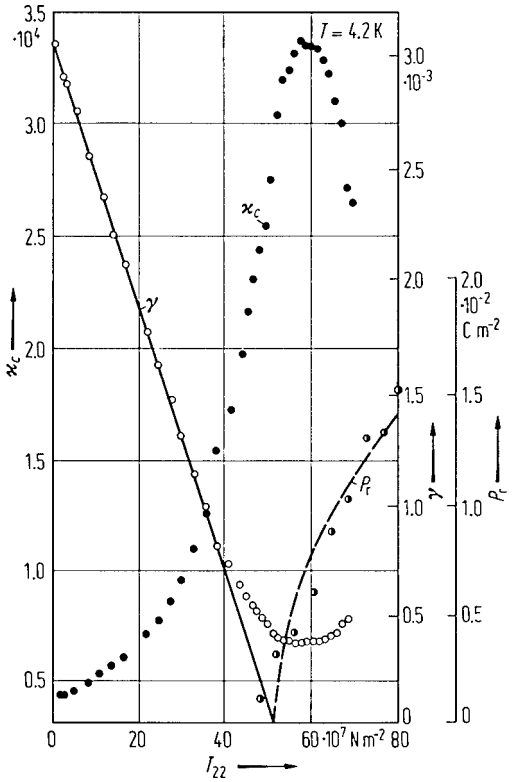

Fig. 1A-5-020. $KTaO_3$. κ_c, γ , P_r vs. T_{22} [73Uwe]. P_r: remanent polarization, $\gamma = 4\pi / (\kappa_c - 1)$: inverse susceptibility in cgs units. T_{22}: uniaxial stress along [010]. κ_c at f = 120 Hz...1 kHz. T = 4.2 K.

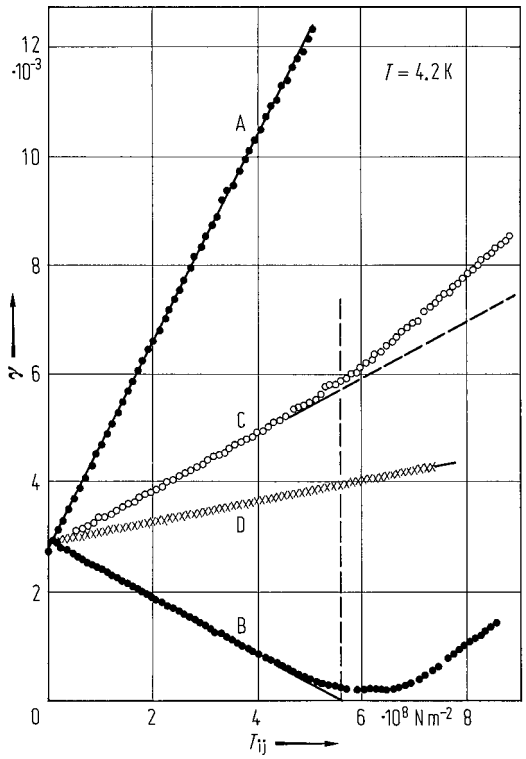

Fig. 1A-5-021. $KTaO_3$. γ vs. T_{ij} [75Uwe]. $\gamma = 4\pi / (\kappa - 1)$; inverse susceptibility in cgs units. T_{ij}: uniaxial stress.

Curve	T_{ij}	direction of measurement
A	⊥(100)	∥ [100]
B	⊥(110)	∥ [001]
C	⊥(110)	∥ [110]
D	⊥(111)	∥ [110]

Vertical dashed line indicates transition stress.

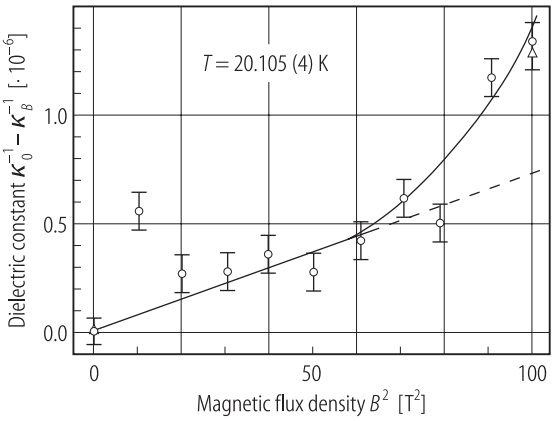

Fig. 1A-5-022. $KTaO_3$. $\kappa_0^{-1} - \kappa_B^{-1}$ vs. B^2 [82Law]. B: magnetic flux density, κ_B: dielectric constant under magnetic field B, κ_0 : dielectric constant at $B = 0$. B is along [111].

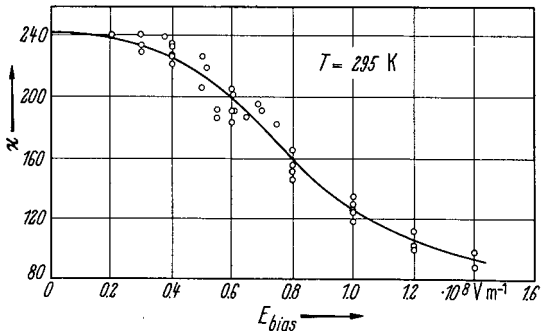

Fig. 1A-5-023. $KTaO_3$. κ vs. E_{bias} [65Kah]. Semiconducting $KTaO_3$ with carrier concentrations $N = 3.5 \cdot 10^{23} ... 1.2 \cdot 10^{25}$ m^{-3} is used for Schottky diode capacitances.

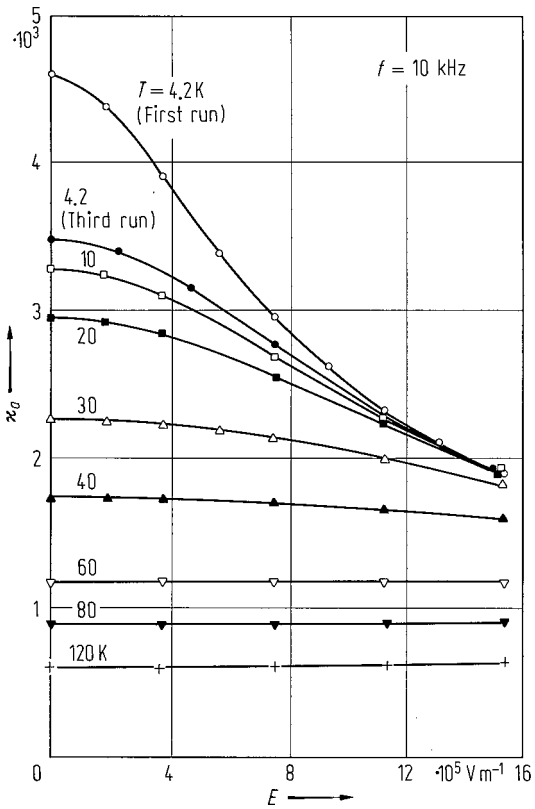

Fig. 1A-5-024. $KTaO_3$. κ_a vs. E [76Fuj1]. Parameter: T.

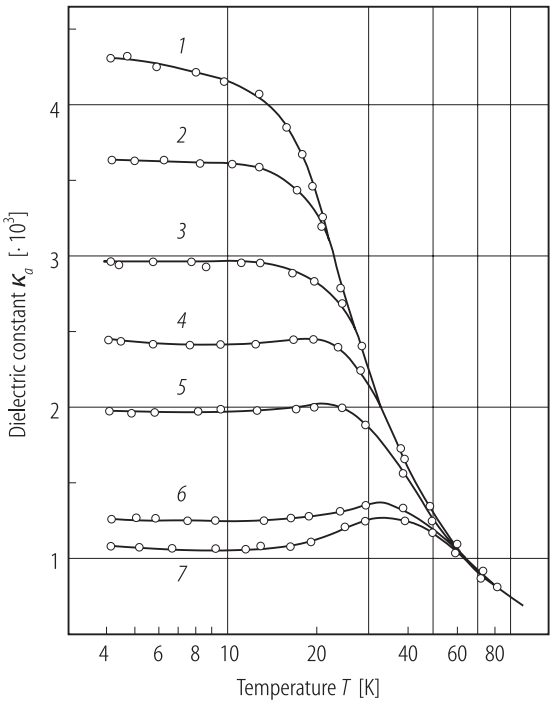

Fig. 1A-5-025. $KTaO_3$. κ_a vs. T [80Buz]. Parameter: E_{bias} along [100]. Curve *1*: E_{bias} = 0 kV/m, *2*: 125 kV/m, *3*: 300 kV/m, *4*: 425 kV/m, *5*: 600 kV/m, *6*: 1000 kV/m, *7*: 1500 kV/m.

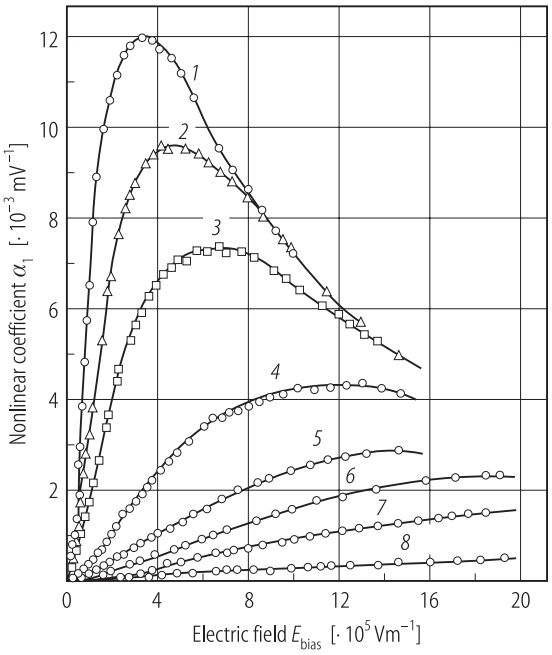

Fig. 1A-5-026. $KTaO_3$. α_1 vs. E_{bias} [80Buz]. α_1: first dynamic nonlinear coefficient of dielectric constant, $\alpha_1 = -(1/\kappa)(\partial\kappa / \partial E)$. Parameter: *T*. Curve *1*: 4.2 K, *2*: 11.1 K, *3*: 17.2 K, *4*: 29.8 K, *5*: 38.6 K, *6*: 45.8 K, *7*: 55.8 K, *8*: 65 K. f = 500 MHz.

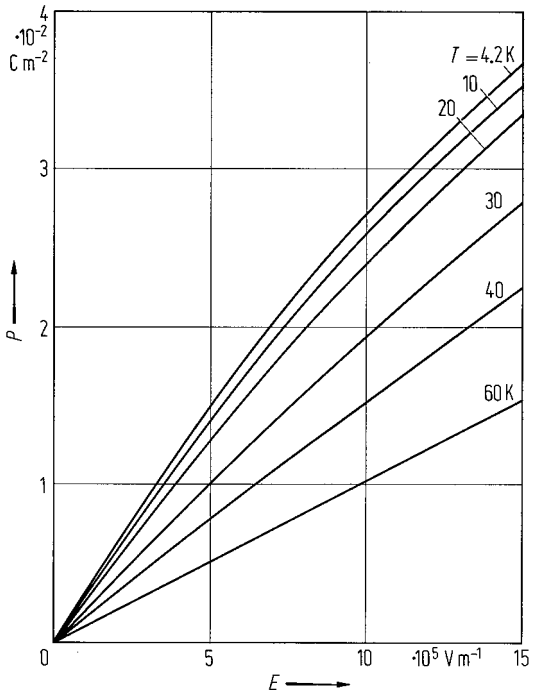

Fig. 1A-5-027. $KTaO_3$. *P* vs. *E* [76Fuj1]. Parameter: *T*.

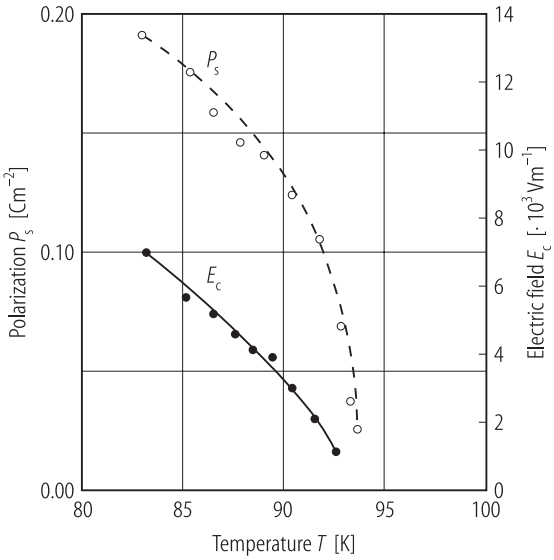

Fig. 1A-5-028. $K_{0.92}Li_{0.08}TaO_3$. P_s, E_c vs. T [92Gli]. From dielectric hysteresis loop. $f < 0.1$ Hz.

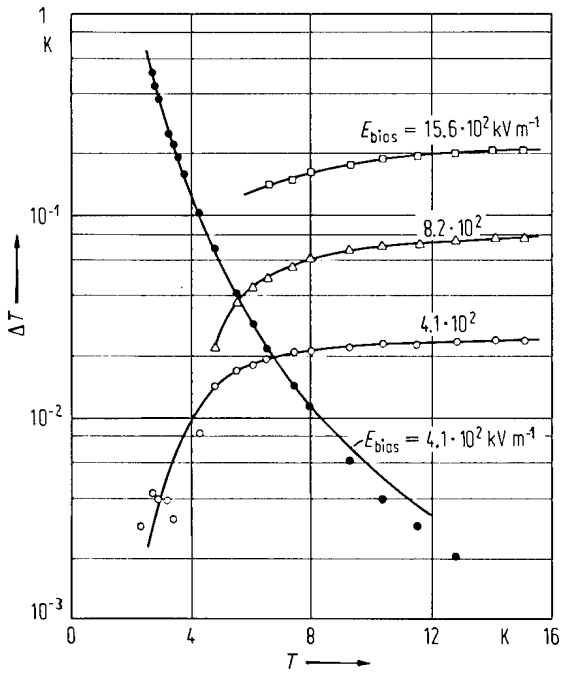

Fig. 1A-5-029. $KTaO_3$. ΔT vs. T [77Law]. Parameter: E_{bias}. ΔT: reversible electrocaloric component (open symbols) and irreversible component (full circles) of the temperature changes.

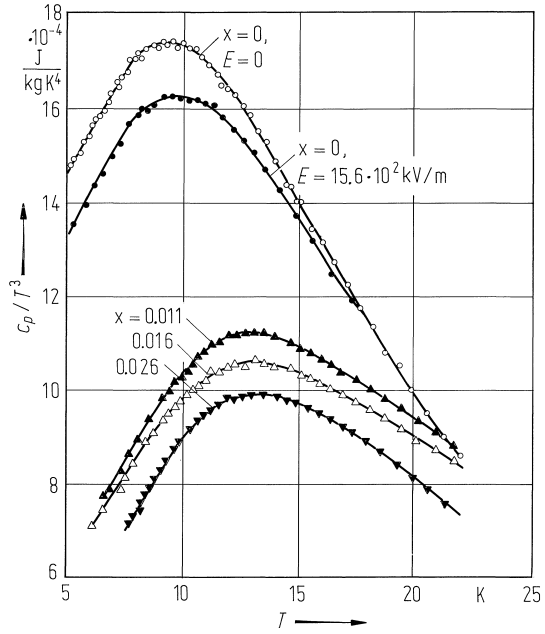

Fig. 1A-5-030. $KTaO_3$, $K_{1-x}Li_xTaO_3$. c_p/T^3 vs. T [84Law]. Parameter: x. E: dc biasing electric field (for only the undoped $KTaO_3$).

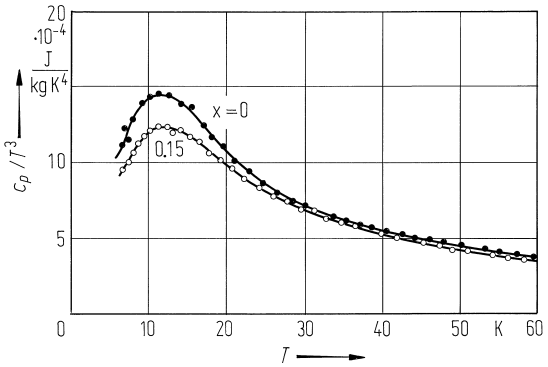

Fig. 1A-5-031. $K_{1-x}Li_xTaO_3$. c_p/T^3 vs. T [86Str].

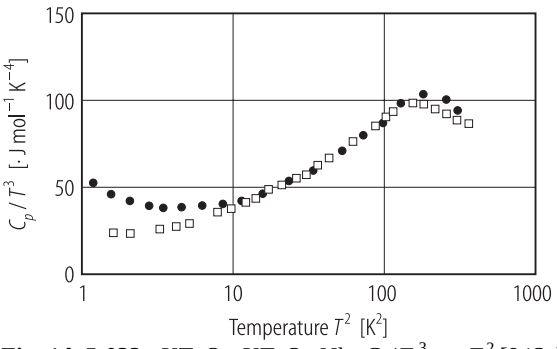

Fig. 1A-5-032. $KTaO_3$, $KTaO_3$:Nb. C_p/T^3 vs. T^2 [94Sal].
Open squares: pure, full circles: 3% Nb doped.

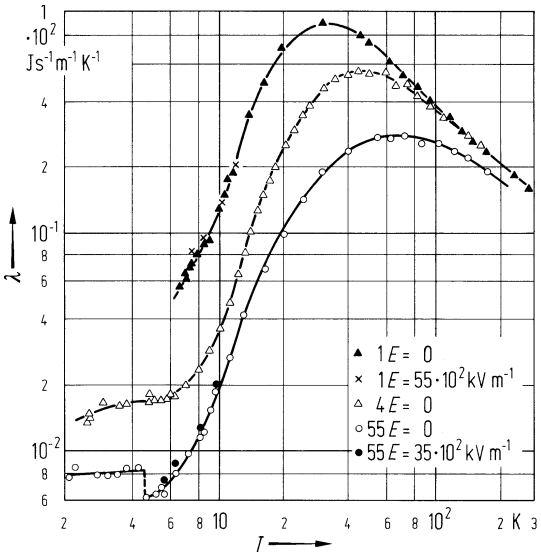

Fig. 1A-5-033. $KTaO_3$. λ vs. T [68Ste]. Parameter: E. λ: thermal conductivity. 1, 4 and 55 in the figure show the sample numbers of the original works.

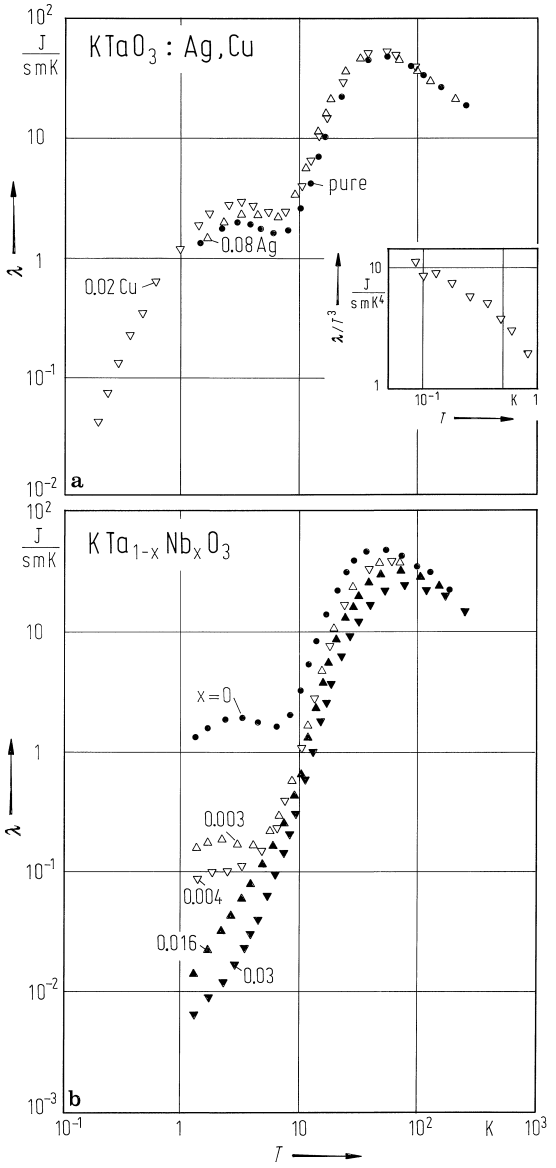

Fig. 1A-5-034. $KTaO_3$, $KTaO_3$:8% Ag, $KTaO_3$:2% Cu, $KTa_{1-x}Nb_xO_3$. λ vs. T [80deG]. λ: thermal conductivity. **(a)** Dopants: Ag or Cu. Insert: λ / T^3 vs. T. **(b)** $KTa_{1-x}Nb_xO_3$. Parameter: x.

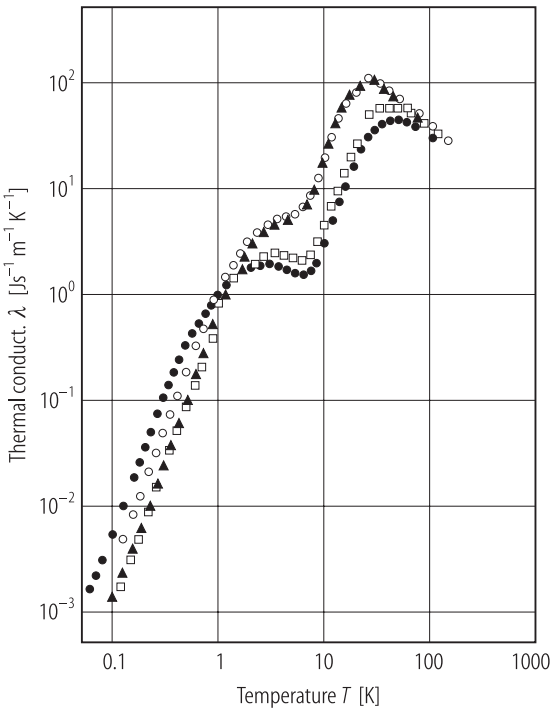

Fig. 1A-5-035. $KTaO_3$. λ vs. T [94Sal]. λ: thermal conductivity. Different symbols in the figure indicate the data of different samples.

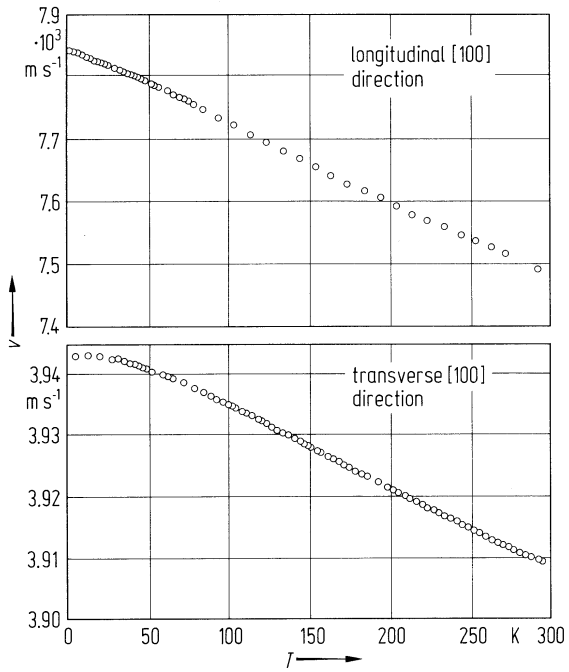

Fig. 1A-5-036. $KTaO_3$. v vs. T [68Bar]. v: velocity of 200 MHz ultrasound wave, propagating along [100].

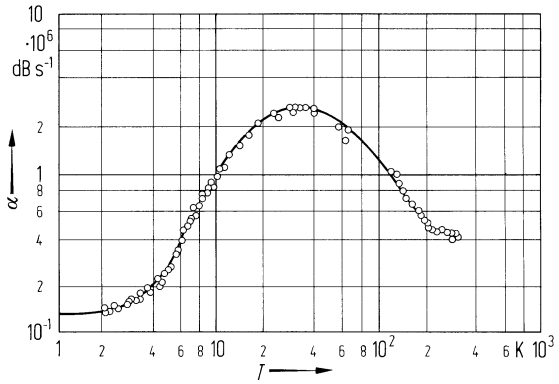

Fig. 1A-5-037. $KTaO_3$. α vs. T [69Bar]. α: ultrasonic attenuation of the longitudinal wave, propagating along [100].

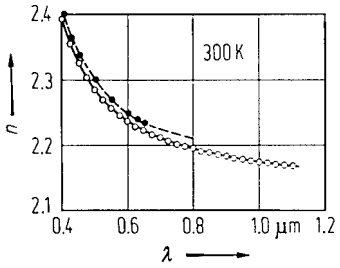

Fig. 1A-5-038. $KTaO_3$. n vs. λ. Solid curve: [76Fuj1], dashed curve: [65Wem].

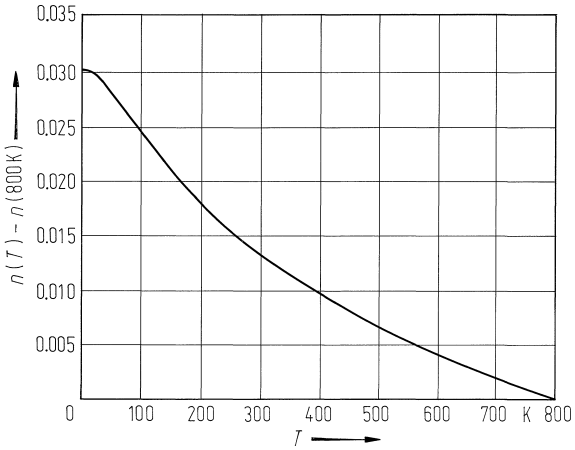

Fig. 1A-5-039. $KTaO_3$. $n(T) - n(800\ K)$ vs. T [85Kle]. $n(T)$: refractive index at T. $\lambda = 589$ nm.

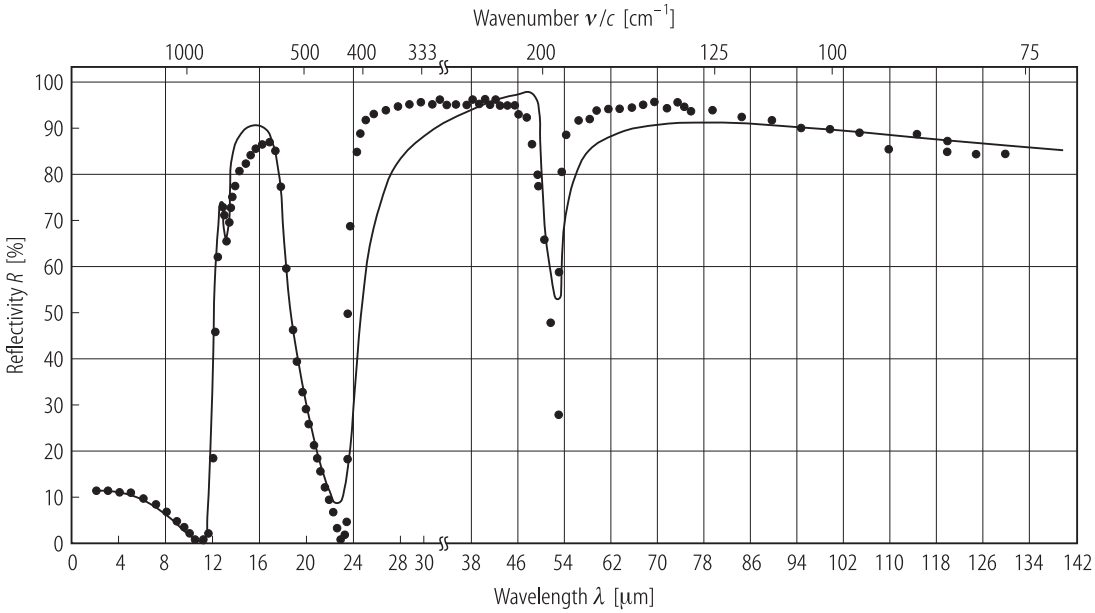

Fig. 1A-5-040. $KTaO_3$. R vs. λ [63Mil]. R: reflectivity. T = RT. Note change of scale at λ = 30 μm.

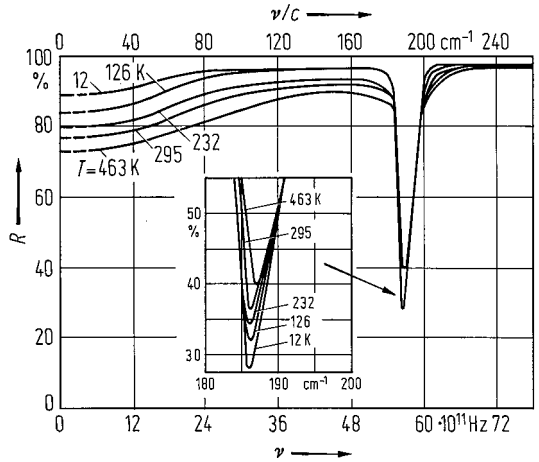

Fig. 1A-5-041. $KTaO_3$. R vs. ν [67Per]. R: reflectivity. Parameter: T.

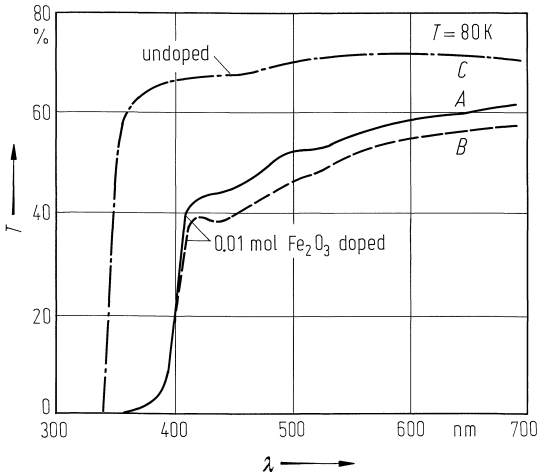

Fig. 1A-5-042. $KTaO_3$ (undoped, Fe doped). *T* vs. λ at 80 K [80Aki]. *T*: transmission. Curve *A*: 0.01 mol Fe_2O_3 doped sample of 1.31 mm thickness, before light irradiation. *B*: after blue light irradiation. *C*: undoped sample of 1.88 mm thickness.

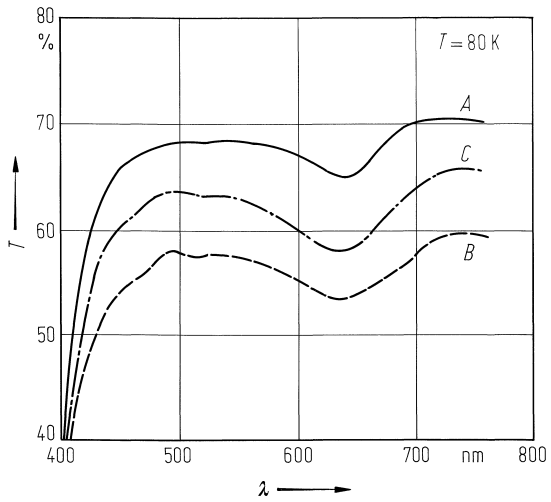

Fig. 1A-5-043. $KTaO_3$ (0.01 mol NiO doped). *T* vs. λ at 80 K [80Aki]. *T:* transmission. Curve *A*: before light irradiation. *B*: after blue light irradiation. *C*: bleached with orange light. Sample thickness 3.88 mm.

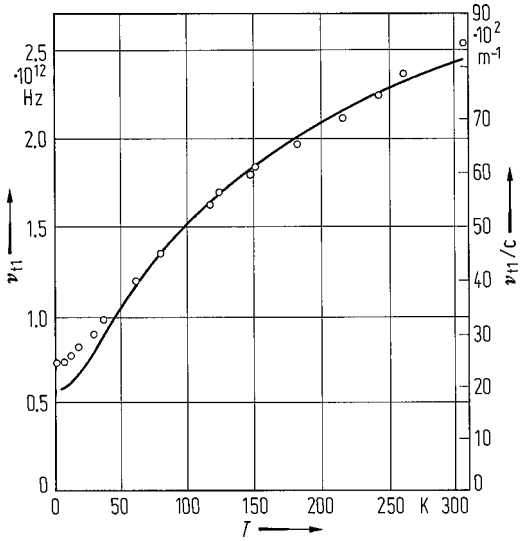

Fig. 1A-5-044. $KTaO_3$. ν_{t1}/c vs. T [67Fle]. ν_{t1}/c: wave number of ferroelectric mode obtained from electric-field induced Raman scattering. Solid line is a plot of $1.28 \cdot 10^3\ \kappa^{-1/2}$.

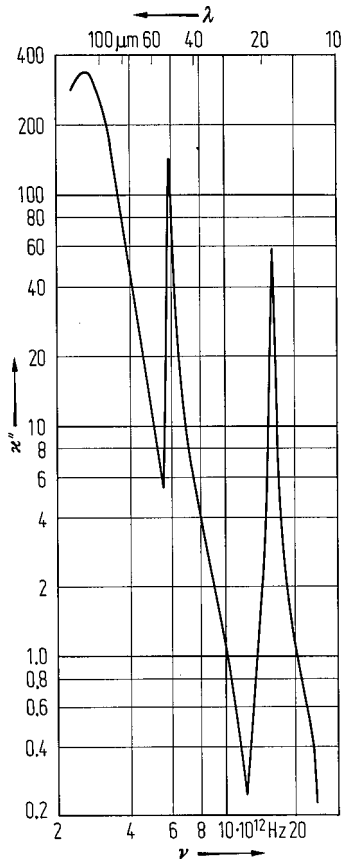

Fig. 1A-5-045. $KTaO_3$. κ'' vs. ν [63Mye]. κ'' was calculated from the reflectivity data. T = RT.